Desalination and Water Treatment
www.deswater.com

doi: 10.5004/dwt.2023.30028

313 (2023) 290–299
November

Coupling coordination analysis between urban park wetland water ecological construction and carbon emissions

Dexin Huang

Anhui Xinhua University, Hefei 230088, China, email: 15156882951@163.com

Received 10 June 2023; Accepted 23 August 2023

ABSTRACT

The low-carbon design of wetland park landscape is very important to maintain the water balance and carbon balance of human and ecosystem. The combination of an increase in carbon emissions and a decrease in carbon capture increases net carbon emissions. Based on the coupling and coordination analysis between water ecological construction and carbon emission of urban park wetland ecological landscape, this study constructed a carbon-water (CW) coupling simulation model of urban park wetland ecological landscape, proposed a low-carbon urban park wetland water ecological model, and then analyzed the coupling effect of carbon and water and carbon emission prediction of urban park wetland. The above method is supported by the recognition technology of CW coupling mechanism of urban park wetland and the reasonable allocation technology of water resources based on low-carbon model, and the technical innovation is realized in these two aspects. Finally, the low-carbon water resource allocation plan of urban park wetland is discussed. The results show that economic development and energy consumption will be developed according to the extended or low-carbon model, and the agricultural and forestry irrigation quota will be reduced by 0.01~0.02 mm and 10,000 m^3 / ha, respectively. The irrigation water utilization coefficient, the water consumption rate of canal system and channel system were increased to 0.74 and 0.85 respectively. The technological innovation and results of this study provide new ideas and methods for low-carbon landscape design and water resource management of wetland landscape ecology.

Keywords: Wetland; Water ecology; Water resource allocation; Carbon emission; Coupling coordination

1. Introduction

Under the background of climate change, environmental ecological problems have evolved into water balance and carbon balance problems of human beings and ecosystems [1]. At present, the world is focusing on the development of carbon emission reduction related research. On the basis of the implementation of ecological planning such as returning farmland to forests, the net carbon emission is still at a high level. The model of "suppressing sources and reducing sinks" is gradually replacing the model of "increasing sources and reducing sinks", and has not yet achieved the transition to the model of "reducing sources and increasing sinks" [2]. Current climate change mitigation measures separate "source reduction" and "sink increase", and have not focused on the extent to which climate change is affected by other greenhouse gases, it was impossible to find the complex causes of "sink reduction" and propose effective "sink increase" measures. It lacked comprehensive regulation of "source reduction" and "sink increase" [3].

The traditional socio-economic demand for water resources is growing, which makes the ecological water use more and more seriously occupied. The economic development has led to the increase of net carbon emissions (CE) [4,5]. Low carbon development mode has become the current main development mode. With the implementation of ecological environment restoration measures, the contradiction between social and environmental water use is constantly being optimized, and gradually tends to "reduce water consumption". Sources increase sinks, but it has not yet reached the ideal state of negative net CE [6]. At present, the discussion of the global "carbon theme" is mainly around the CO_2 concentration, and the analysis of the "water problem" is based on the shortage of fresh water. These basic studies provide a theoretical basis for relevant research in the ecological field [7].

How to adjust the relationship between carbon "source/sink" and water use, and reduce the net CE through water resource allocation has become an important research direction in the field of ecological environment research. Yao and Song [8] studied CH_4 and CO_2 in wetland ecosystem and analyzed potential emission factors. The research results highlight the emission characteristics of CH_4 and CO_2 under various water levels, providing a theoretical basis for wetland restoration. Bonetti et al. [9] learned from the analysis that, after 20 y of restoration, the results show that the fence restoration of semi-arid rain irrigated wetland has almost no impact on microbial dynamics and carbon process. This study will help relevant scholars to design the most effective wetland restoration measures. Were et al. [10] analyzed the impact of paddy wetland on climate, and compared the CO_2 and CH_4 fluxes in different seasons. The results showed that the CO_2 flux of paddy fields in dry and rainy seasons was significantly higher than that of vegetation communities in natural profiles; and it was predicted that the future emissions of CO_2 and CH_4 from wetlands in the study area would mainly come from paddy wetlands, and had faster expansion rate.

This study constructed the wetland water ecological environment in urban parks, analyzed the coupling and coordination between CE, expanded the theory of wetland water resource allocation, linked the carbon cycle with the water resource system, and realized the technology of water resources to cope with climate change. Innovation, especially providing technical support for climate change mitigation. Taking an urban wetland park as an example, this study will coordinate the relationship between the society and ecology to meet the multi-dimensional goals of economic development, carbon emission reduction, ecological environment protection, wetland habitat maintenance, and groundwater level restoration. practical significance.

2. Process simulation of carbon and water coupling elements in urban park wetland landscape

2.1. The general idea of ecological landscape simulation modeling

Carbon water (CW) coupling simulation is an important part of eco-hydrological simulation. It is also a key technology for water resources and ecological assessment, which meets the requirements of water resources planning and ecological planning [11,12]. The CW coupling model mainly focuses on energy flow, natural social water cycle, and carbon cycle process. Energy processes affect the flux and stock of CW cycle elements, such as photosynthetically active radiation that directly affects net primary productivity, and determines the sensitivity of evapotranspiration. heat, latent heat, and changes in canopy air domain, vegetation, and soil temperature; with the continuous development of social economy, ecological water use is affected by social water use, resulting in changes in CE and carbon capture processes. Therefore, water intake, factors such as water delivery, water use, drainage, and recycled water utilization are taken into account in the water cycle; The wetland park is dominated by the wetland ecological environment, with water as the landscape matrix and water and land transition zone as the characteristics. After continuous succession and evolution, the habitats are stable and diverse, and the biological populations including plants and animals are very rich, and the plant landscape is rich and varied, and flexible animals travel through it. CE, carbon dioxide emissions from vegetation, capture processes, allometric growth of vegetation itself, and soil decomposition processes have become the focus of carbon cycle research.

2.2. Simulation of elements and processes in wetland park design

Energy flow, water cycle, and carbon cycle are the key factors in the CW coupling model [13]. The energy flow mainly analyzes the surface radiation process, sensible heat, latent heat and soil heat flux; the carbon cycle mainly analyzes the social and economic CE, as well as the productivity generation, material distribution, and decomposition of organic matter in the ecosystem; The natural water cycle mainly analyzes the processes of snow accumulation and snowmelt, soil water process, and surface runoff; the social water cycle mainly analyzes the historical data of water resource use in the region [14]. For specific simulation methods, Table 1.

3. Construction of urban park wetland water ecology under low carbon

3.1. Ecological landscape model construction method

Wetland park is a wetland landscape area with the functions of species and habitat protection, ecological tourism and ecological education. The construction of wetland landscape should take wetland protection and restoration as the premise, and pay attention to the principle of ecological protection. Water resources allocation is the key technology for carrying out water resources planning, implementing comprehensive regulation and scientific management of regional water resources [15]. RAWRLC is a water resource allocation model with multiple water sources, multiple users, and multiple control elements [16]. The model uses modular programming technology to integrate the data pre-processing simulation module, optimization simulation module and post-processing module; among them, the optimization simulation module is the core module of the model [17]. The data pre-processing simulation module mainly includes the format processing of long series of water supply and demand data, carbon emission and carbon capture data, and the operation and scheduling rules of water conservancy projects; the data post-processing module is formatted and output according to user needs, including different optimal simulation results of actual water supply, water consumption, water shortage rate, CE, carbon capture, and net CE in regions and different water users [18]. Among them, the carbon capture of the configuration unit needs to be calculated in combination with the spatiotemporal statistical results of the daily output data of the carbon cycle simulation model, as shown in Fig. 1.

3.2. Objective function and constraint analysis of landscape security pattern

Select the water shortage and net carbon emission as the key target factors. Let the minimum function of water shortage of the unit be expressed as $f_1(x)$; the minimum function of the net carbon emission of the unit is expressed as $f_2(x)$; the minimum value of the difference between the net CE of adjacent units is $f_3(x)$; the minimum function of the difference between adjacent units' water shortage is $f_4(x)$.

Table 1
Simulation methods for elements of energy flow, carbon cycle and water cycle

Thread	Element process		Simulation method
Energy flow	Long wave radiation		Law of energy balance
	Shortwave radiation		
	Sensible heat flux		Canopy and surface energy balance
	Latent heat flux		
	Soil heat flux		Calculation by capacity, thickness, temperature, etc.
Carbon cycle	Artificial	Carbon emission	Carbon emission coefficient method
	Natural	Net primary productivity	Simulate respiration and photosynthesis
		Material distribution	Increment distribution in blade, sapwood and root
		Material circulation	Calculation according to the life value of leaves, sapwood and roots of vegetable type
		Death	Considering the natural and stress death of fallen leaves
		Decomposition of soil organic matter	Considering temperature, soil moisture content and decomposition time
Water cycle	Natural	Snow melting	Temperature index method
		Surface runoff	Houghton slope runoff
		Infiltration	Green Ampt model
		Soil water movement	Havercamp, Mualem formula
		Groundwater movement	Bouusinessq equation, Darcy's law, etc.
		Swallow hair	Penman Monteith formula
		Slope confluence	Kinematic wave model
		River confluence	Kinematic wave model and dynamic wave model
	Artificial	Water intake, transmission, consumption and drainage	Statistic historical data and assign weights

$$\begin{cases} f = \left\{ f_1(x), f_2(x), f_3(x), f_4(x) \right\} \\ f_1(x) = \min \sum_{t=1}^{T} \sum_{m=1}^{M} W(t,m,x) \\ f_2(x) = \min \sum_{t=1}^{T} \sum_{m=1}^{M} C_{\text{net}}(t,m,x) \\ f_3(x) = \min \left| \Delta C_{\text{net}} \right| = \min \left| C_{\text{net}}(t,m+1,x) - C_{\text{net}}(t,m,x) \right| \\ f_4(x) = \min \left| \Delta W \right| = \min \left| W(t,m+1,x) - W(t,m,x) \right| \end{cases} \quad (1)$$

where t is the period, m is the calculation unit, and x is the water supply. It $W(t,m,x)$ is the water shortage of the x first time m period t; it is ΔW the $W(t,m,x)$ difference between adjacent configuration units; x it $C_{\text{net}}(t,m,x)$ is the net carbon emission of ΔC_{net} the first time m period: t the difference $C_{\text{net}}(t,m,x)$ between two adjacent calculation units during the time period t. The constraints on the total amount of wetland water consumption are shown in Eq. (2).

$$\sum W_{\text{con}}(t) \le W_{\text{avail}}(p) \quad (2)$$

where $W_{\text{con}}(t)$ t is the amount of water resources that can be consumed at time; p is the frequency of incoming water; $W_{\text{avail}}(p)$ is the amount of water resources that can be consumed at time p. The calculation of unit water balance constraints is shown in Eq. (3).

$$W(t,m,x) = \sum_{n=1}^{N} k_1(n) \begin{pmatrix} W_{\text{demand}}(t,m,n) - W_{\text{rivers}}(t,m,n) \\ -W_{\text{reseviors}}(t,m,n) - W_{\text{undergs}}(t,m,n) \\ -W_{\text{reuses}}(t,m,n) - W_{p\,\&\,\text{fs}}(t,m,n) \end{pmatrix} \quad (3)$$

where $k_1(n)$ is the weight of the total water demand of the calculation unit, $W_{\text{demand}}(t,m,n)$, $W_{\text{rivers}}(t,m,n)$, $W_{\text{reseviors}}(t,m,n)$, $W_{\text{undergs}}(t,m,n)$, $W_{\text{reuses}}(t,m,n)$, $W_{p\&\text{fs}(t,m,n)}$ are the water demand, river water supply, reservoir water supply, groundwater water supply, reclaimed water reuse, and rain and flood resources of the calculation unit in period t, respectively. The balance calculation formula of reservoir water volume is shown in Eq. (4).

$$\text{VR}(t+1,r) = \text{VR}(t,r) + \Delta\text{VR}(t,r) - \text{VRD}(t,r) - \text{VRL}(t,r) \quad (4)$$

where VR(t,r) and VR(t + 1,r) are the initial and final storage capacities of the r reservoir hub in case of t, respectively; ΔVR(t,r), VRD(t,r) and VRL(t,r) are respectively the storage change, discharge volume and water loss of the r reservoir when t. For the carbon balance constraint process, set $C_{\text{net}}(t,m,x)$ x the net CE as follows, Eq. (5) t m.

$$\begin{aligned} C_{\text{net}}(t,m,x) &= C_{\text{release}}(t,m,x) - C_{\text{capture}}(t,m,x) \\ &= \sum_{n=1}^{N} C_{\text{release}}(t,m,x,n) - \sum_{p=1}^{q} C_{\text{capture}}(t,m,x,p) \le 0 \end{aligned} \quad (5)$$

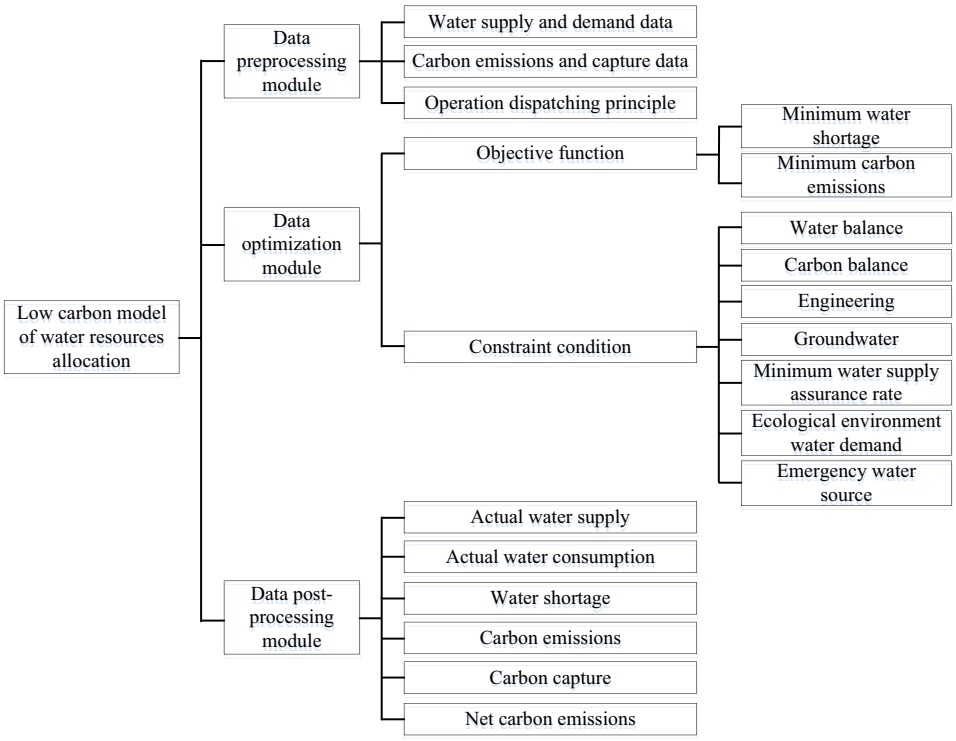

Fig. 1. Wetland water resources allocation model under low-carbon mode.

where $C_{release}(t,m,x)$, $C_{capture}(t,m,x)$ are respectively x the carbon emission and carbon capture in the $C_{release}(t,m,x,n)$ following t time. m, $C_{capture}(t,m,x,p)$ are respectively x the CE and carbon captures of the following industries, Eq. (6) m n t.

$$\begin{cases} C_{capture}\left(t,m,x,p\right)=\mathrm{NPP}_{d}\left(m,x,p\right)\times t_{turn} \\ \mathrm{NPP}_{d}\left(m,x,p\right)=28.5\begin{pmatrix}\Delta h/24\times A\left(\boldsymbol{m},x,p\right)\\ -\mathrm{Ra}\left(m,x,p\right)\end{pmatrix} \\ \times 0.5\times 10^{-6}\times 86400 \end{cases} \tag{6}$$

where $\mathrm{NPP}_{d}(m,x,p)$ represents x the daily net primary productivity kg·C of each carbon "sink" at the p next t time, and the unit is m; t_{turn} represents the time conversion coefficient between time t and day; Δh represents m the p sunshine hours of each carbon "sink" $A(m,x,p)$; represents x the p next m. The photosynthesis rate of the carbon "sink", in unit μmol(CO_2/m^2·s); Ra(m,x,p) x the vegetation respiration rate of the next carbon "sink", μmol(CO_2/m^2·s); p other m constants represent the conversion coefficient of carbon. CW relationship index constraints, Eq. (7).

$$\begin{cases} \mathrm{NRW}\left(t,m,x\right)=\mathrm{RW}\left(t,m,x\right)-\mathrm{CW}\left(t,m,x\right) \\ \mathrm{RW}\left(t,m,x\right)=\dfrac{C_{release}\left(t,m,x\right)}{W_{s}\left(t,m,x\right)}=\sum_{n=1}^{N}\dfrac{C_{release}\left(t,m,x,n\right)}{W_{s}\left(t,m,x,n\right)}\le \mathrm{RW}_{max} \\ \mathrm{CW}\left(t,m,x\right)=\dfrac{C_{capture}\left(t,m,x\right)}{W_{s}\left(t,m,x\right)}=\sum_{p=1}^{q}C_{capture}\left(t,m,x,p\right)/ \\ \qquad\qquad \sum_{n=1}^{N}W_{s}\left(t,m,x,n\right)\le \mathrm{CW}_{min} \end{cases} \tag{7}$$

where NRW(t,m,x) represents x the net emission benefit of unilateral water and carbon in the following time; RW(t,m,x), t, m, respectively CW(t,m,x) represent $W_s(t,m,x)$ the x carbon emission benefit, carbon capture benefit, and water consumption of unilateral water and carbon in the following time; RW_{max}, t are m, respectively CW_{min} the m carbon emission benefit of unilateral water and carbon The maximum value and the minimum value of carbon capture benefit. For the calculation of carbon emission capture effect, Eq. (8).

$$\begin{cases} \mathrm{PRC}_{pri}\left(t,m\right)=C_{pri\_release}\left(t,m\right)/W_{pri}\left(t,m\right)\le \max \mathrm{PRC}_{pri} \\ \mathrm{PCC}_{pri}\left(t,m\right)=C_{pri\_capture}\left(t,m\right)/W_{pri}\left(t,m\right)\le \min \mathrm{PCC}_{pri} \end{cases} \tag{8}$$

where pri represents $\mathrm{PRC}_{pri}(t,m)$ the carbon emission and capture benefits of water $W_{pri}(t,m)$ conservancy projects, pri, $\mathrm{PCC}_{pri}(t,m)$, respectively. t m, $C_{pri\_release}(t,m)$, $C_{pri\_capture}(t,m)$ are t the wading volume, carbon emission benefit and carbon capture benefit of the project, respectively; $\max\mathrm{PRC}_{pri}$, m are the $\min\mathrm{PCC}_{pri}$ historical sequence maximum value and $C_{pri\_capture}(t,m)$ historical sequence minimum value of unilateral water, respectively. $C_{pri\_release}(t,m)$ For the calculation of groundwater level constraints, Eq. (9).

$$\mathrm{Ug}_{min}\left(t,m\right)\le \mathrm{Ug}\left(t,m\right)\le \mathrm{Ug}_{max}\left(t,m\right) \tag{9}$$

where $\mathrm{Ug}_{min}(t,m)$, $\mathrm{Ug}(t,m)$, $\mathrm{Ug}_{max}(t,m)$ are t m the shallowest groundwater depth, groundwater depth, and deepest groundwater depth, respectively. For the calculation of the minimum water supply guarantee rate constraint, Eq. (10).

$$s_1(t,m,n) \geq s_{\min}(t,m,n) \tag{10}$$

where $s_1(t,m,n)$ and $s_{\min}(t,m,n)$ are the assurance rate of water supply and the minimum assurance rate of water supply for the n industry of m in case of t. The ecological water demand constraint on the slope is shown in Eq. (11).

$$\mathrm{Wsed}(t,m,k) \geq \mathrm{Wsed}_{\min}(t,m,k) \tag{11}$$

where $W\mathrm{sed}(t,m,k)$, $W\mathrm{sed}_{\min}(t,m,k)$ are the actual value and the minimum value of the ecological water requirement t m of the first k kind of slope, respectively. Constraints on river ecological flow process, Eq. (12).

$$\mathrm{Wred}(t,m) \geq \mathrm{Wred}_{\min}(t,m) \tag{12}$$

where $W\mathrm{red}(t,m)$, are $W\mathrm{red}_{\min}(t,m)$ the actual value and the minimum value of the ecological water requirement of the river in time, respectively. t m Eq. (13) for environmental water constraints.

$$\mathrm{Wevd}(t,m) \geq \mathrm{Wevd}_{\min}(t,m) \tag{13}$$

where $W\mathrm{evd}(t,m)$, $W\mathrm{evd}_{\min}(t,m)$ are t m the actual value and the minimum value of environmental water demand, respectively.

For the solution of the model, the genetic algorithm is used to calculate $f_i(x)$, and calculate the optimal solution f_i^* of each goal function. Then the shortest distance from the ideal point is calculated $\min\phi[f(x)]$, and finally the satisfactory solution is calculated through the genetic algorithm [19].

4. Coupling effect of carbon and water in urban park wetlands and prediction of CE

4.1. CW coupling mechanism

This study takes a certain Yanghu Wetland Park as an example. The park is divided into wetland ecological community, wetland ecological conservation area, wetland biodiversity display area, public service area, wetland science and education area and wetland ecological corridor. The greening rate is as high as 70%, and the negative oxygen. The ion content is 6 times higher than that of the central city. Based on the concept system of wetland CW coupling, according to the needs of CW coupling simulation and rational allocation of water resources, explore the internal relationship between key elements in the watershed CW cycle, especially the relationship between natural water cycle and carbon capture, as well as the relationship between social water cycle and CE relationship.

Fig. 2 shows the precipitation inspection results of the wetland park. Taking the precipitation from 1971 to 2020 as the basic data, the Mann–Kendall method was used to test, and it was found that the mutation point of 2005–2015 was between 2007–2010, as shown in Fig. 2a. Tested by the Multimedia Mass Transfer model (MMT) method, it is found that the mutation point is located in 2009–2010, as shown in Fig. 2b. Comparing the results of the two tests, it can be seen that the abrupt change point of precipitation first appeared from 2005 to 2010, and the precipitation gradually decreased after 2015. Therefore, the verification period and verification period of water cycle are set as 2005–2010 and 2011–2015, respectively.

Taking the monthly runoff data of three hydrological stations from 2005 to 2015 as the research object, the relative error between the simulated and measured runoff values and the Nash–Sutcliffe efficiency were selected (Table 2).

The leaf area index was selected for verification, and field investigations were carried out in spring, summer and autumn. Among the measured and simulated values, the relative error of about 73% observation points is within 40%, as shown in Fig. 3. It can be seen from the measured results in Fig. 3 that only 27% of the measured values have a relative error of more than 40%, and most of the measured values are similar to the simulated values. This result is acceptable due to the larger model cells.

The characterization of wetland CW coupling quantitative relationship mainly includes three aspects, namely carbon emission coefficient, capture coefficient and net emission coefficient. According to the data from 2015 to 2020, the value of each coefficient can be obtained, as shown in Fig. 4. Among the carbon emission coefficients, the average values of social economy, production, and living carbon emission coefficients are 0.0078, 0.0076 and 0.0084 t/m^3, respectively. Showing an increasing trend, Fig. 4a. The average carbon capture coefficient of wetland area from 2015 to

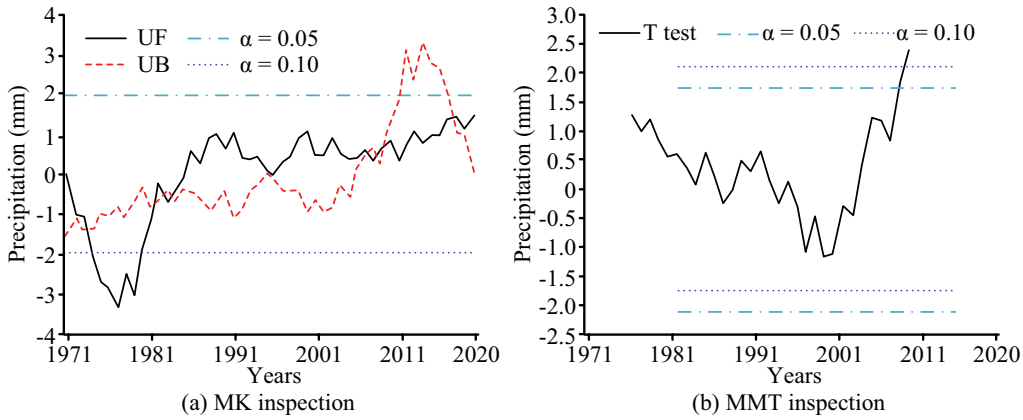

(a) MK inspection (b) MMT inspection

Fig. 2. (a) Mann–Kendall inspection and (b) MMT inspection.

Table 2
Water cycle calibration results

Time	Parameter	Hydrometric station 1	Hydrometric station 2	Hydrometric station 3
Calibration period (2005~2010)	Relative error	0.20	0.23	0.27
	Nash coefficient	0.96	0.85	0.84
Validation period (2011~2015)	Relative error	0.12	0.18	0.43
	Nash coefficient	0.95	0.94	0.67

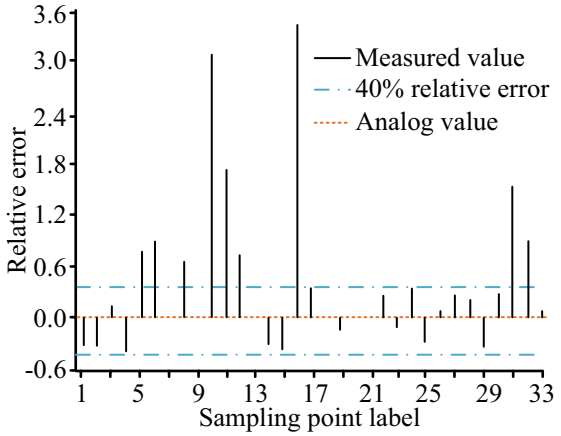

Fig. 3. Leaf area index relative error of sampling point.

2020 was 0.0012 t/m^3, which decreased by 61.2% compared with 2015 in 2020, but since 2016, the carbon capture coefficient of wetland area has shown a rising trend, as shown in Fig. 4b. The average net emission coefficient of carbon in the wetland area from 2015 to 2020 was 0.0067 t/m^3, moreover, since 2015, the net carbon emission coefficient of wetland area has shown a growing trend as a whole. Compared with 2015, it has increased by 159.3% in 2020, as shown in Fig. 4c.

4.2. Carbon emission prediction model construction

According to the formula in the IPCC guidelines, the t calculation method of wetland CE in the first year is obtained [20], Eq. (14).

$$\mathrm{Ce}_i = \sum_{j=1}^{4} E(t) q_{ij} c_j \tag{14}$$

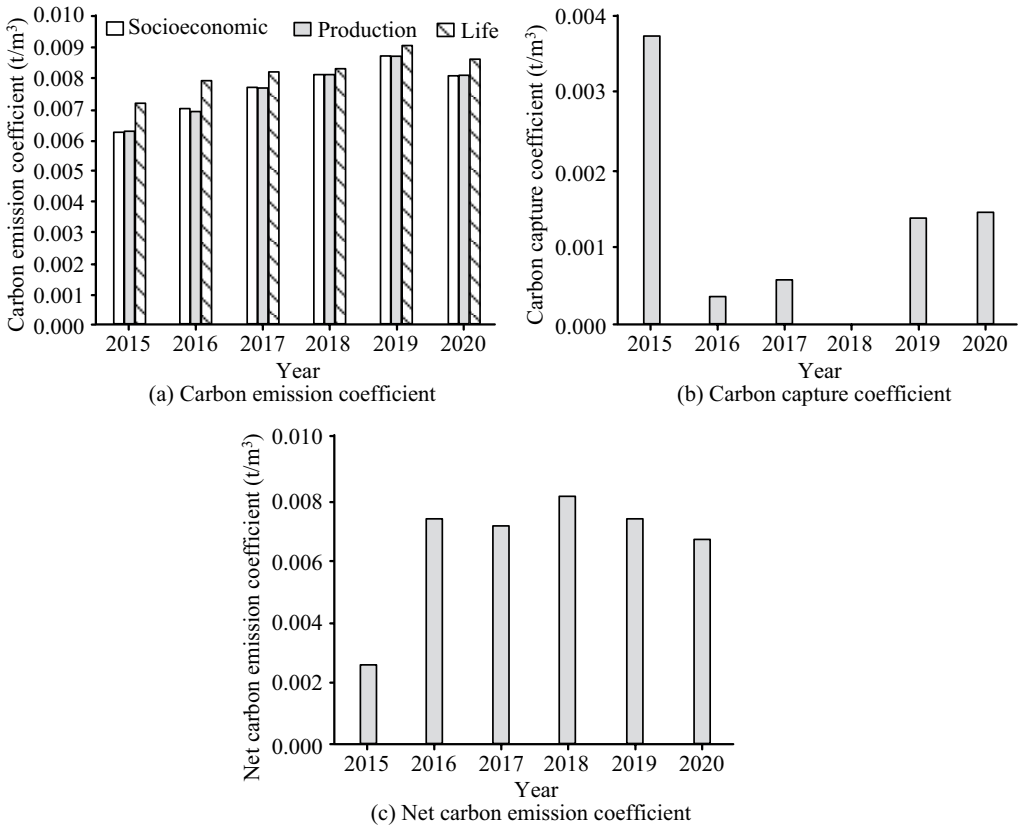

Fig. 4. Quantitative relationship of wetland carbon water coupling. (a) Carbon emission coefficient, (b) carbon capture coefficient and (c) net carbon coefficient.

where Ce_i represents t the carbon emission of the year, c_j represents j the CE coefficient of the type energy, and q_{ij} represents the proportion of type j energy efficiency in year t. Gross production value of wetlands and capital stock can be converted into comparable prices in 2010 [20–23], Eq. (15).

$$K_t = K_{t-1}\left(1-\delta_t\right) + I_t \tag{15}$$

where K_t, K_{t-1} represent t the capital stock in the δ_t year and year, respectively, and t–1 represent the economic depreciation rate, which is 9.6% according to previous research. Suppose the energy intensity is $\tau(t)$, the initial annual energy intensity is τ_0, and the growth rate of energy intensity is v_τ [24–27], Eq. (16).

$$\ln\tau\left(t\right) = \ln\tau_0 + v_\tau t + \varepsilon \tag{16}$$

where ε represents the error term. The energy intensity of wetlands is calculated by local energy consumption and GDP data, and linear regression fitting is carried out [28–31] (Table 3).

The linear regression result is good, R^2 = 0.948, and the v_τ is –0.03, so the fitting model is shown in Eq. (17).

$$\tau\left(t\right) = 2.035\times e^{-0.03t} \tag{17}$$

Through Eq. (17) it can be concluded that the annual decline rate of energy intensity is 3%. Further calculate the economic changes through the optimization model of the dynamic relationship, assuming that the t number of employees in the year is $L(t)$ [32,33], the linear statistical model is shown in Eq. (18).

$$\ln\left(\frac{Y\left(t\right)}{E\left(t\right)}\right) = \ln A_0 + \alpha\ln\left(\frac{K\left(t\right)}{E\left(t\right)}\right) + \gamma\ln L\left(t\right) + vt + \varepsilon \tag{18}$$

After linear regression analysis through SPSS, the optimal economic growth parameters can be obtained, as shown in Table 4. The linear regression result is good, R^2 = 0.995, except for γ, the significance test of other parameter levels is less than 0.05, which indicates that other parameter levels are significant.

Therefore, the dynamic relationship model is modified to obtain the calculation Formula of the optimal economic growth rate [34,35], as shown in Eq. (19).

$$\begin{cases} Y\left(t\right) = Ae^{vt}K\left(t\right)^{\alpha}E\left(t\right)^{1-\alpha}, \quad 0<A<1, \quad 0<\alpha<1 \\ g\left(t\right) = -\left(1/\delta\right)\left[\rho-\left(\varepsilon-\theta\tau\left(t\right)\right)\left(A_0e^{vt}\right)^{1/\alpha}\tau\left(t\right)^{1-\alpha}\right] \end{cases} \tag{19}$$

Table 3
Parameter estimation of energy intensity

Parameter	Parameter value	T	Level of significance
$\ln\tau(t)$	0.72	44.575	0.000
v_τ	–0.03	12.706	0.000

If the derivative of energy intensity is 0, then when the growth rate is maximum and optimal, the energy intensity relationship is shown in Eq. (20).

$$\tau_{\max} = \frac{\varepsilon\left(1-\alpha\right)}{\theta} \tag{20}$$

where $\tau_{\max}$ represents the maximum energy intensity of the wetland from 2010 to 2020, and the value of the variable θ is 24.757. According to the constraints, the adjustment parameter can be δ 8.904, which ϱ is –0.830.

Based on the extended development model, the benchmark year is set as 2020, and the energy intensity and economic growth rate are 1.42 t/10,000 yuan and 12.3%, respectively. The results of 2025, 2030 and 2040 are calculated based on the above data. The results show that the carbon emission in 2025 will increase by 87.29% compared with that in 2020, but on the whole, the energy intensity of wetlands will continue to decline, and the energy consumption will increase significantly.

According to the energy intensity, energy consumption and energy structure, it is predicted that the CE in 2025, 2030 and 2040 will be 0.004912, 0.005805 and 0.007059 Mt, respectively, with an increase of 34.5%, 58.9% and 93.35% compared with 2020. Although the energy intensity and the proportion of low-carbon energy have decreased, due to the rigid demand of economic development for energy, the CE will still show an increase trend by 2040, but the increase rate will decrease, Table 5.

4.3. Prediction and analysis of water demand in wetland park landscape

Based on the natural monthly runoff data from 2000 to 2010, the average runoff flow in the driest month of each year is selected, and then the monthly runoff Q_{m90} and the

Table 4
Estimation of economic parameters

Parameter	Parameter value	T	Level of significance
$\ln(A_0)$	1.667	4.496	0.003
v	0.010	2.583	0.034
α	0.488	6.016	0.000
γ	0.098	0.572	0.587

Table 5
Prediction of energy consumption, carbon emissions and energy intensity

/	2025	2030	2040
Energy consumption (Mt sce)	0.0991	0.17699	0.56458
Carbon emissions (Mt)	0.0684	0.12217	0.38968
Energy intensity (t/10,000 yuan)	1.27	1.09	0.81
Optimal economic growth rate (%)	8.24	6.92	5.26
GDP (RMB100mn)	0.59298	0.84561	0.149433
Energy consumption (Mt sce)	0.0746	0.0916	0.1199

annual average monthly diameter with a frequency of 90% are calculated, respectively. The flow Q_{ave} is based on the principle of ensuring that the river does not flow, and the monthly average water demand quota Q_{em} is selected, Table 6.

Therefore, it can be calculated that the annual ecological water demand of the upstream river in the wetland is 21,400 m^3, and the annual ecological water demand is only 13,600 m^3 based on 90% monthly runoff. On the premise of ensuring the water level, considering various ecological indicators comprehensively, the monthly average water level guarantee rate is between 65% and 75%, and the annual ecological water demand of the wetland is 47,200 and 38,900 m^3, respectively. The water demand for wetland ecological environment in 2015, 2020 and 2030 is shown in Table 7.

4.4. Water allocation plan for Wetland Park

The rational allocation plan of urban wetland water resources based on the low-carbon development model is mainly set from five aspects: social and economic development, water supply model, water use model and water conservancy project layout.

4.4.1. Base year 2020

After understanding the water shortage rate and net carbon emission level of wetland ecological water demand; agricultural irrigation quota, industrial GDP added value water consumption and domestic water quota will be reduced by 15%, and irrigation water utilization rate and canal water utilization rate will be increased by 5%, respectively. %, reduce groundwater supply. The scheme adopts a high water-saving scheme.

Table 6
Monthly average water demand quota of wetland rivers (10,000 m^3)

Parameter	Q_{m90}	Q_{ave}	Q_{em}
River 1	0	0.053	0.053
River 2	0.0419	0.1019	0.0419
River 3	0.0589	0.0935	0.0589
River 4	0	0.002	0.002
River 5	0.0718	0.1544	0.0718
River 6	0	0.0047	0.0047

Table 7
Water demand for ecological environment (10,000 m^3)

Region		Wetland
Current level	2025	1.5040
	2030	1.7883
	2040	2.5885
Planning level	2025	1.2533
	2030	1.4902
	2040	2.1571

4.4.2. Horizontal year 2025

This scheme is a high water-saving scheme, the average agricultural irrigation quota is reduced to about 0.117 mm, and the forestry irrigation quota is reduced to 3,400 m^3/ha. At the same time, the utilization coefficient of irrigation water and the utilization rate of canal water were increased to 0.74 and 0.85, respectively.

4.4.3. Horizontal year 2030

This scheme is a high water-saving scheme, and the agricultural and forestry irrigation quotas are reduced by 0.01 mm and 0.2 million·m^3/ha, respectively; the irrigation water utilization coefficient and the canal water utilization ratio are increased to 0.74 and 0.85, respectively.

4.4.4. Horizontal year 2040

This scheme is a high water-saving scheme, and the fixed amount of agricultural and forestry irrigation is further reduced by 0.01 mm and 0.1 million·m^3/ha; the irrigation water utilization coefficient and the canal water utilization ratio are increased to 0.74 and 0.85, respectively.

5. Conclusion

For an urban wetland park, a reasonable allocation scheme of water resources based on low carbon model in different levels of years in the future is proposed, and the following conclusions are drawn:

First, based on the extended development model, the benchmark year is set as 2020, using the relevant data of 2020. The energy intensity and economic growth rate are respectively 1.42 t/10,000 yuan and 12.3%. Based on the above data, the wetland energy consumption and CE in 2025, 2030 and 2040 are calculated. The results show that CE will increase by 87.29% in 2025 compared to 2020, but the overall energy intensity of wetlands shows a continuous downward trend, and energy consumption has increased significantly.

Second, according to energy intensity, energy consumption and energy structure, the CE in 2025, 2030 and 2040 are predicted to be 0.004912, 0.005805 and 0.007059 Mt, respectively, an increase of 34.5% and 58.9% compared with 2020 and 93.35%. Although energy intensity and the proportion of low-carbon energy have decreased, due to the rigid demand for energy in economic development, CE will still increase by 2040, but the rate of increase will decrease.

Thirdly, the urban wetland water resource allocation scheme under the low-carbon model is proposed. (a) Base year is 2020. Understand the water shortage rate and net carbon emission level of wetlands after ecological water demand; The agricultural irrigation quota, water consumption of industrial GDP added value and domestic water quota will be further reduced by 15%, and the utilization rate of irrigation water and canal system water will be increased by 5%, respectively, to reduce groundwater supply. The scheme adopts a high-water saving scheme. (b) Horizontal year 2025. This scheme is a high water-saving scheme, the average agricultural irrigation quota is reduced to about 0.117 mm, and the forestry irrigation quota is reduced to 3,400 m^3/ha.

At the same time, the utilization coefficient of irrigation water and the utilization rate of canal water were increased to 0.74 and 0.85, respectively. (c) Horizontal year 2030. This scheme is a high water-saving scheme, and the agricultural and forestry irrigation quotas are reduced by 0.01 mm and 0.2 million·m^3/ha, respectively; the irrigation water utilization coefficient and the canal water utilization ratio are increased to 0.74 and 0.85, respectively. (d) Horizontal year 2040. This scheme is a high water-saving scheme, and the fixed amount of agricultural and forestry irrigation is further reduced by 0.01 mm and 0.1 million·m^3/ha; the irrigation water utilization coefficient and the canal water utilization ratio are increased to 0.74 and 0.85, respectively.

To sum up, the low-carbon design of wetland water environment in urban park provides a water source guarantee for the construction of wetland landscape, and is also the ecological environment basis for creating good wetland landscape effect. This low-carbon design not only helps to improve the efficient use of water resources, but also helps to achieve the coordinated development of ecological and economic objectives. This finding highlights the importance of low-carbon strategies in water resource management and ecological conservation in urban wetland parks.

Funding

This research is supported by: A research project on the innovation and development of social science in Anhui Province in 2021: "Research on Wetland Landscape Planning in the Ecological Demonstration Zone of Huanchao Lake under the Background of Dual Carbon (Project No. 2021CX146)".

References

[1] Y. Yang, X. Mou, B. Wen, X. Liu, Soil carbon, nitrogen and phosphorus concentrations and stoichiometries across a chronosequence of Restored Inland Soda Saline-Alkali Wetlands, Western Songnen Plain, Northeast China, Chin. Geogr. Sci., 30 (2020) 934–946.

[2] A.L. Hinson, R.A. Feagin, M. Eriksson, Environmental controls on the distribution of tidal wetland soil organic carbon in the Continental United States, Global Biogeochem. Cycles, 33 (2019) 1408–1422.

[3] J.G. Ochoa-Gómez, S.E. Lluch-Cota, V.H. Rivera-Monroy, D.B. Lluch-Cota, E. Troyo-Diéguez, W. Oechel, E. Serviere-Zaragoza, Mangrove wetland productivity and carbon stocks in an arid zone of the Gulf of California (La Paz Bay, Mexico), For. Ecol. Manage., 442 (2019) 135–147.

[4] D. Xiao, L. Deng, D.-G. Kim, C. Huang, K. Tian, Carbon budgets of wetland ecosystems in China, Global Change Biol., 25 (2019) 2061–2076.

[5] L.G. Chambers, H.E. Steinmuller, J.L. Breithaupt, Toward a mechanistic understanding of "peat collapse" and its potential contribution to coastal wetland loss, Ecology: Ecol. Soc. America, 100 (2019) e02720, doi: 10.1002/ecy.2720.

[6] S.R. Padhy, P. Bhattacharyya, P.K. Dash, K.S. Roy, S. Neogi, M.J. Baig, P. Swain, A.K. Nayak, T. Mohapatra, Enhanced labile carbon flow in soil-microbes-plant-atmospheric continuum in rice under elevated CO_2 and temperature leads to positive climate change feed-back, Appl. Soil Ecol., 155 (2020) 103657, doi: 10.1016/j.apsoil.2020.103657.

[7] A.L. Ganesan, A.C. Stell, N. Gedney, E. Comyn-Platt, G. Hayman, M. Rigby, B. Poulter, E.R.C. Hornibrook, Spatially resolved isotopic source signatures of wetland methane emissions, Geophys. Res. Lett., 45 (2018) 3737–3745.

[8] X. Yao, C. Song, Effect of different factors dominated by water level environment on wetland carbon emissions, Environ. Sci. Pollut. Res., 29 (2022) 74150–74162.

[9] G. Bonetti, S.M. Trevathan-Tackett, P.E. Carnell, S. Treby, P.I. Macreadie, Local vegetation and hydroperiod influence spatial and temporal patterns of carbon and microbe response to wetland rehabilitation, Appl. Soil Ecol., 163 (2021) 103917, doi: 10.1016/j.apsoil.2021.103917.

[10] D. Were, F. Kansiime, T. Fetahi, H. Thomas, Carbon dioxide and methane fluxes from a tropical freshwater wetland under natural and rice paddy conditions: implications for climate change mitigation, Wetlands Global Change, 41 (2021) 1–12, doi: 10.1007/s13157-021-01451-4.

[11] L. Huo, Y. Zou, X. Lyu, Z. Zhang, X. Wang, Y. An, Effect of wetland reclamation on soil organic carbon stability in peat mire soil around Xingkai Lake in Northeast China, Chin. Geogr. Sci., 28 (2018) 325–336.

[12] L. Wei, Z. Zhu, S. Liu, M. Xiao, J. Wang, Y. Deng, Y. Kuzyakov, J. Wu, T. Ge, Temperature sensitivity (Q_{10}) of stable, primed and easily available organic matter pools during decomposition in paddy soil, Appl. Soil Ecol., 157 (2021) 103752, doi: 10.1016/j.apsoil.2020.103752.

[13] Y. Liu, M. Jiang, X. Lu, Y. Lou, B. Liu, Carbon, nitrogen and phosphorus contents of wetland soils in relation to environment factors in Northeast China, Wetlands, 37 (2017) 153–161.

[14] G. Bonetti, S.M. Trevathan-Tackett, P.E. Carnell, S. Treby, P.I. Macreadie, Local vegetation and hydroperiod influence spatial and temporal patterns of carbon and microbe response to wetland rehabilitation, Appl. Soil Ecol., 163 (2021) 103917, doi: 10.1016/j.apsoil.2021.103917.

[15] Y. Guan, J. Bai, X. Tian, L. Zhi, Z. Yu, Integrating ecological and socio-economic systems by carbon metabolism in a typical wetland city of China, J. Cleaner Prod., 279 (2021) 123342, doi: 10.1016/j.jclepro.2020.123342.

[16] C.D. Ficken, S.J. Connor, R. Rooney, D. Cobbaert, Drivers, pressures, and state responses to inform long-term oil sands wetland monitoring program objectives, Wetlands Ecol. Manage., 30 (2022) 47–66.

[17] H. Sun, Q. Xin, Z. Ma, S. Lan, Effects of plant diversity on carbon dioxide emissions and carbon removal in laboratory-scale constructed wetland, Environ. Sci. Pollut. Res. Int., 26 (2019) 5076–5082.

[18] H. Yang, X. Chen, J. Tang, L. Zhang, C. Zhang, D.C. Perry, W. You, External carbon addition increases nitrate removal and decreases nitrous oxide emission in a restored wetland, Ecol. Eng., 138 (2019) 200–208.

[19] J. Jia, H. Jian, D. Xie, Z. Gu, C. Chen, Multi-scale decomposition of energy-related industrial carbon emission by an extended logarithmic mean Divisia index: a case study of Jiangxi, China, Energy Effic., 12 (2019) 2161–2186.

[20] A. Song, X. Yang, X. Zhang, F. Wang, W. Huang, Ecology environment research about carbon emission efficiency in China based on a novel super epsilon-based measures (SEBM) model, Appl. Ecol. Environ. Res., 17 (2019) 1109–1128.

[21] T. Peng, H. Deng, Research on the sustainable development process of low-carbon pilot cities: the case study of Guiyang, a low-carbon pilot city in south-west China, Environ. Dev. Sustainability, 23 (2021) 2382–2403.

[22] M. Du, J. Antunes, P. Wanke, Z. Chen, Ecological efficiency assessment under the construction of low-carbon city: a perspective of green technology innovation, J. Environ. Plann. Manage., 65 (2022) 1727–1752.

[23] V.W.Y. Tam, K.N. Le, C.N.N. Tran, I.M.C.S. Illankoon, A review on international ecological legislation on energy consumption: greenhouse gas emission management, Int. J. Construct. Manage., 21 (2021) 631–647.

[24] Y. Chen, H. Lu, J. Li, J. Xia, Effects of land use cover change on carbon emissions and ecosystem services in Chengyu urban agglomeration, China, Stochastic Environ. Res. Risk Assess., 34 (2020) 1197–1215.

[25] S.A.R. Shah, S.A.A. Naqvi, S. Anwar, Exploring the linkage among energy intensity, carbon emission and urbanization in Pakistan: fresh evidence from ecological modernization and

environment transition theories, Environ. Sci. Pollut. Res., 27 (2020) 40907–40929.
[26] H. Jiang, J. Peng, J. Dong, Z. Zhang, Z. Xu, J. Meersmans, Linking ecological background and demand to identify ecological security patterns across the Guangdong-Hong Kong-Macao Greater Bay Area in China, Landscape Ecol., 36 (2021) 2135–2150.
[27] Y. Sun, L. Qian, Z. Liu, The carbon emissions level of China's service industry: an analysis of characteristics and influencing factors, Environ. Dev. Sustainability, 24 (2022) 13557–13582.
[28] C. Sun, The correlation between green finance and carbon emissions based on improved neural network, Neural Comput. Appl., 34 (2022) 12399–12413.
[29] J. Wang, C.W. Yu, S.-J. Cao, Technology pathway of efficient and climate-friendly cooling in buildings: towards carbon neutrality, Indoor Built Environ., 30 (2021) 1307–1311.
[30] Q. Li, The view of technological innovation in coal industry under the vision of carbon neutralization, Int. J. Coal Sci. Technol., 8 (2021) 1197–1207.
[31] X. Lyu, A. Shi, X. Wang, Research on the impact of carbon emission trading system on low-carbon technology innovation, Carbon Manage., 11 (2020) 183–193.
[32] K. Zickfeld, D. Azevedo, S. Mathesius, H. Damon Matthews, Asymmetry in the climate–carbon cycle response to positive and negative CO_2 emissions, Nat. Clim. Change, 11 (2021) 613–617.
[33] K. Liu, Y. Qiao, T. Shi, Q. Zhou, Study on coupling coordination and spatiotemporal heterogeneity between economic development and ecological environment of cities along the Yellow River Basin, Environ. Sci. Pollut. Res., 28 (2021) 6898–6912.
[34] Y. Zhou, Y. Kong, T. Zhang, The spatial and temporal evolution of provincial eco-efficiency in China based on SBM modified three-stage data envelopment analysis, Environ. Sci. Pollut. Res., 27 (2020) 8557–8569.
[35] M. Aydin, Y.E. Turan, The influence of financial openness, trade openness, and energy intensity on ecological footprint: revisiting the environmental Kuznets curve hypothesis for BRICS countries, Environ. Sci. Pollut. Res., 27 (2020) 43233–43245.